CEA/DAPNIA/SEA-98-42

RF Kick Measurement on TTF and Comparison with the TESLA Specifications

S. Fartoukh, M. Jablonka, O. Napoly,
DAPNIA/SEA, CEA/Saclay F-91191 Gif sur Yvette Cedex, France
T. Garvey, LAL 91405 Orsay Cedex, France
H. Weise, DESY, Notkesstrasse 85, 22603 Hamburg, Germany

September 17, 1998

Abstract

The accelerating RF field in TESLA cavities presents asymmetries around the cavity axis, due to the input couplers, which give transverse RF deflections (RF kicks) to the beam. These deflections can induce non-negligible vertical emittance dilution of the TESLA beam. A beam experiment on the TESLA Test Facility (TTF) has been dedicated to the measurement of their magnitude. We report on the results from this experiment and compare them to the theoretical expectations as well as to TESLA tolerances.

1 Introduction and recalls

Due to the input couplers, the accelerating RF field in TESLA cavities presents asymmetries around the cavity axis, which give transverse RF deflections to the beam. Since these deflections can induce some vertical emittance dilution of the TESLA beam, a beam experiment on the TESLA Test Facility (TTF) has been dedicated to the measurement of their magnitude. After a rapid description of the experiment, we will report the main results of measurements made on the eight cavities of the first module of the TTF linac (Section 2) and compare them, on the one hand, to theoretical values obtained from a 3D-simulation of the input coupler region and, on the other hand, to the TESLA tolerances relative to both the CDR and the high luminosity beam parameters (Section 3). The detailed description of the experiment can be found in Ref. [1]; its main features are reported hereafter.
The problem is to separate the effects generated by cavity misalignments from those due to couplers. It can then be shown that the first ones are independent of the sign of the RF phase $\phi_{\rm rf}$ with respect to the beam, whereas the second ones contain an out-of-phase component [1]. Moreover, since the HOM couplers are quasi un-coupled to the RF power transported by the accelerating fundamental mode, their effects are negligible compared to the ones generated by the input couplers. The transverse (say horizontal) kick $\delta x'$ given to the beam at the exit of each cavity can then be split into two distinct components: $\delta x' = \delta x'_1(\phi_{\rm rf}) + \delta x'_2(\phi_{\rm rf})$ where $\delta x'_1$ (misalignment contribution) is an even function of the RF phase, and $\delta x'_2$ (input coupler contribution) is proportional to the accelerating gradient $G_{\rm rf}$ of the cavity considered and has the following form [2]:

$$\delta x'_2(\phi_{\rm rf}) = T_x \frac{\Delta E_0}{E_f} \cos(\phi_{\rm rf} + \phi_0) \tag{1}$$

with the following notations :

• $\Delta E_0 = qG_{\rm rf}L$ is the maximum voltage gain within the cavity of length L, and $E_f = E_i + \Delta E_0 \cos(\phi_{\rm rf})$ is the beam energy at the cavity exit where the input coupler is located.

• $\phi_0 = \omega_{\rm rf} s_0/c \sim 157.7°$ is a phase shift linked to the distance $s_0 = 10.1$ cm from the center of the cavity end-cell to the center of its input coupler.

• T_x [rad] quantifies the magnitude of the RF kick and is the relevant quantity to be measured. Its theoretical value has been estimated to 0.18 mrad [2] (see Section 3). Note that the factor T_y is theoretically zero since the input coupler lies in the horizontal plane and does not break the symmetry $y \leftrightarrow -y$.

Consequently, by monitoring the transverse beam displacement at the end of the linac, say $dx(\phi_{\rm rf})$ as a function of the RF phase of the selected cavities, and by considering its anti-symmetrical part, i.e. the function $dx^-(\phi_{\rm rf}) = \Big[dx(\phi_{\rm rf}) - dx(-\phi_{\rm rf})\Big]$, the misalignment contribution disappears naturally and the values of T_x and T_y can be measured.
The experimental protocol is then the following:

- select one or several cavities in the first TTF cryomodule ACC1.

- keep the accelerating gradient constant within the whole module (by fixing the klystron power) and vary the RF phases ϕ_{rf_i} of the selected cavities.
- measure the change in the beam position at the end of the first module.

Measuring the average effect of the 8 cryomodule cavities powered by a single klystron can be easily done in practice by changing the global phase of the klystron. A necessary prerequisite is however that, for a given phase of the klystron, the beam is on crest in each cavity to a precision of a few degrees. This was achieved by careful tuning of the electrical length of the individual cavity wave guides.
Measuring the RF-steering effect of a given cavity was thought to be doable by detuning all other cavities, and controlling the phase of this cavity with the klystron phase. It was realized later that even if the accelerating field does not fill the 7 detuned cavities, it is still present at the level of their input coupler and thus affects the validity of the measurement [3].
Finally, the possibility to act individually on the RF phase of a single cavity (the seven others being tuned and powered) by adjusting step by step the electrical length of its wave guide had been given up because it would have required a tunnel access before each measurement.
We therefore report only on the measurement of the average effect of the 8 cavities.

2 Measurement

During the measurements, the beam initial energy (at the exit of the capture cavity) was approximatively $E_0 = 9.5$ MeV and the accelerating gradient was fixed to $G_{\mathrm{rf}} = 13$ MeV/m in the 8 cavities. The cold doublet FACC1 being switched off, the beam position was measured by the RF-BPM located at the end of section BC1, i.e. approximatively 11.7 m downstream from the last cavity exit.
The values of the klystron phase have been taken in a range of 50° around a central value corresponding to an on-crest acceleration, i.e. $-25° \leq \phi_{\mathrm{rf}} \equiv \phi_{\mathrm{rf}_1} = \ldots = \phi_{\mathrm{rf}_8} \leq 25°$.
The horizontal and vertical beam positions measured at the BPM location are plotted in Fig. 1 with respect to the klystron phase. The anti-symmetrical parts of these curves are shown in Fig. 2 (black dots). The fits of these experimental points represented in dot-dashed lines on this same figure have been obtained in the following way:

1. by assuming the coupler effects to be of same magnitude in all the cavities (which has to be approximatively the case since they depend only on the coupler and cavity geometry), i.e. $T_{x,y_i} \equiv T_{x,y}$, $i = 1 \ldots 8$.

2. by taking the analytical form of the RF kick given by Eq. 1.

3. by computing at the BPM location the anti-symmetrical part of the transverse beam displacement generated by these kicks:

$$dx^{-}(\phi_{\mathrm{rf}}) = \Big[dx(\phi_{\mathrm{rf}}) - dx(-\phi_{\mathrm{rf}})\Big] \;\text{ with }\; dx(\phi_{\mathrm{rf}}) = T_x\; q\, G_{\mathrm{rf}}\, L \sum_{i=1}^{8} \frac{R_{12}(i;\phi_{\mathrm{rf}})}{E_f(i;\phi_{\mathrm{rf}})} \qquad (2)$$

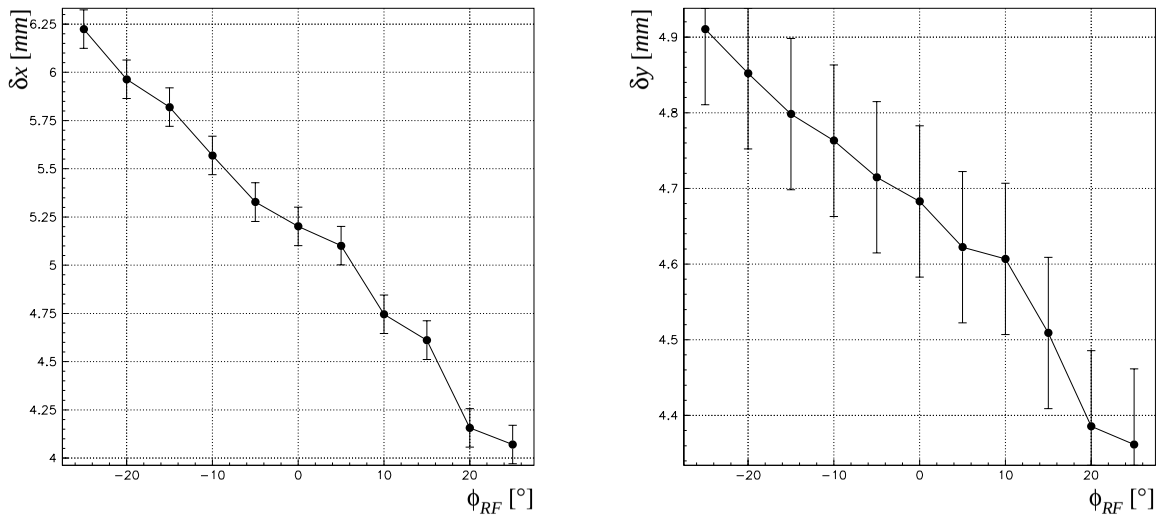

(a) (b)

Figure 1: Horizontal (a) and vertical (b) beam displacements read at BPM versus $\phi_{\rm rf}$; error bars of $\pm 100\,\mu$m taking into account the BPM resolution and the pulse to pulse jitter.

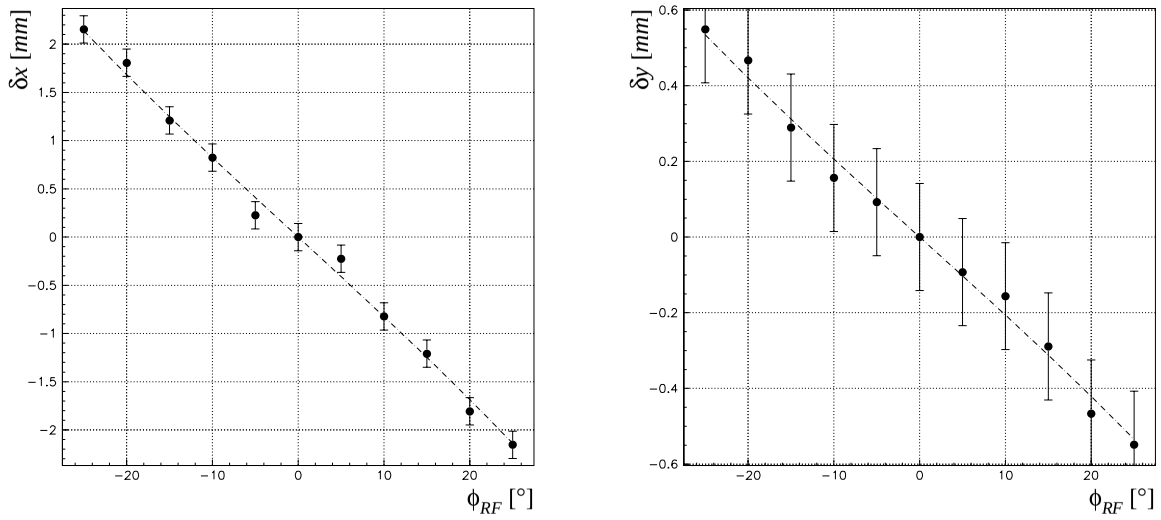

(a) (b)

Figure 2: Anti-symmetrical part of the horizontal (a) and vertical (b) beam displacements versus $\phi_{\rm rf}$; experimental points (black dots) and fits (dot-dashed lines); error bars of $\pm 100\sqrt{2}\,\mu$m taking into account the BPM resolution and the pulse to pulse jitter.

where $R_{12}(i;\phi_{\rm rf})$ is the coefficient (1,2) of the transfer matrix from the exit of the cavity number i to the BPM center (taking into account the rf-focusing effects in the cavities $i+1,\ldots,8$) and where $E_f(i;\phi_{\rm rf}) = E_0 + i \times qG_{\rm rf}L\cos(\phi_{\rm rf})$ represents the beam energy at the exit of this same cavity.

The cavity averaged T factors obtained by this method are the following:

$$T_x = \mathbf{0.32 \pm 0.03}\ \text{mrad} \quad \text{and} \quad T_y = \mathbf{0.08 \pm 0.03}\ \text{mrad}\,.$$

The 2-σ uncertainty of 0.03 mrad on these values takes into account the systematic errors of measurement ($\pm 100\,\mu$m RMS containing both the BPM resolution and the pulse to pulse jitter) as well as the errors on the estimation of gradients $G_{{\rm rf}_i}$ and RF phases $\phi_{{\rm rf}_i}$ of the eight ACC1 cavities (± 2.5 % FW for the gradients and $\pm 2^\circ$ RMS for the phases).

3 Expected theoretical values and comparison with the TESLA specifications

3.1 Theoretical values expected for the factors T_x and T_y

As expected, the horizontal effect is larger than the vertical one. A possible explanation for the measured non-zero T_y value may be a cell-to-cell vertical displacement abnormally large for one or several cavities of the module which, consequently, would break the symmetry $y \leftrightarrow -y$ (for instance cavity sag due to gravity); another one may be the small coupling of the HOM couplers to the accelerating mode. Although the measured value, as discussed in the next section, is smaller than the specifications required for TESLA, investigation of the vertical effect deserves further study.
Concerning the horizontal effect, the value of the kick P_x [eV/c] given at the cavity exit has been estimated in a recent paper [2] from a semi-analytical approach of the problem combined with a 3-D simulation of the electro-magnetic field generated in the region of the input coupler:

$$P_x = m_e\gamma c\delta x' = \frac{q\,\alpha_E\,\hat{E}_z\,d}{c}\,\frac{3/\pi}{1-(3d/\lambda)^2}\left[-\cos(\pi\frac{3d}{2\lambda}) + \alpha_B\sin(\pi\frac{3d}{\lambda})\right]\cos(\phi_{\rm rf}+\phi_0) \qquad (3)$$

where the notations have the following meanings:

- $d = 4$ cm represents the outer diameter of the input coupler, $\lambda \approx 23$ cm is the RF wave length and $\phi_0 = 157.7^\circ$ is the phase shift occurring in Eq. 1.
- $\hat{E}_z \equiv 2\,G_{\rm rf}$ is the peak accelerating gradient.
- $\alpha_E \equiv \dfrac{\hat{E}_x}{\hat{E}_z} \approx \dfrac{10^3}{4Q_l} = 1.39\,10^{-4}$ and $\alpha_B \equiv \dfrac{c\hat{B}_y}{\hat{E}_x} \approx 0.075\,(2+10^{-4}Q_l) = 13.65$ for $Q_l = 1.8\,10^6$

(Q-loaded factors of ACC1 cavities) where $\hat{E}_x$ and $\hat{B}_y$ are the peak values of the horizontal electrical and vertical magnetic fields in the coupler region.

With our notations, this corresponds to

$$T_x = \frac{2\,\alpha_E\,d}{L}\,\frac{3/\pi}{1-(3d/\lambda)^2}\left[-\cos(\pi\frac{3d}{2\lambda})+\alpha_B\sin(\pi\frac{3d}{\lambda})\right] \sim \mathbf{0.18}\ \text{mrad} \qquad (4)$$

for a cavity of electrical length $L = 9\lambda/2 = 1.0385$ m.

3.2 Tolerance specifications for TESLA

	Ref. design	**Stage-II**
Bunch charge N_e [10^{10}]	3.63	2.00
Bunch length σ_z [mm]	0.7	0.4
Injection energy E_0 [GeV]	3.2	3.9
Initial uncoherent energy spread $\sigma_{\delta_{\text{uncoh.}}}$ [%]	1	1
Normalized emittances $\epsilon_{x,y}$ [10^{-6} m]	14/0.25	10/0.03
Accelerating gradient G_{rf} [MeV/m]	25	25
Rf phase w.r.t. the beam ϕ_{rf} [°]	3.4	4.1
Final energy E_f [GeV]	250.51	251.27
Final energy spread (RMS) σ_δ [10^{-4}]	3.6	2.6
Final total energy spread $(\Delta E/E)_{\text{tot}}$ [%]	0.45	0.34

Table 1: CDR (ref. design) and high luminosity (stage-II) single-bunch parameters for TESLA 500 [4] (the charge distribution of the bunch as well as its initial energy distribution are truncated at $\pm 3\,\sigma$).

In order to specify the tolerances on T_x and T_y for TESLA cavities, we use two different beam parameter sets: the so-called "CDR" and "high luminosity" parameters relative to the 500 GeV version of TESLA and reported in Tab. 1 [4]. Considering the same linac optics as the one described in Ref. [5, p.387] [1] and a perfectly aligned machine, the vertical (resp. horizontal) single-bunch emittance has been computed at the linac exit for different values of T_y (resp. T_x) and assuming a "one-to-one" algorithm to correct the off-axis beam trajectories. The results obtained for the two parameter sets are shown in Figs. 3 and 4 respectively. Small relative emittance growths can be parameterized as

$$\begin{cases} \dfrac{\Delta\epsilon_x}{\epsilon_x} = 5\%\left(\dfrac{T_x\,[\text{mrad}]}{2.64}\right)^2 \text{ and } \dfrac{\Delta\epsilon_y}{\epsilon_y} = 5\%\left(\dfrac{T_y\,[\text{mrad}]}{0.31}\right)^2 \text{ for the CDR parameters} \\ \dfrac{\Delta\epsilon_x}{\epsilon_x} = 5\%\left(\dfrac{T_x\,[\text{mrad}]}{5.19}\right)^2 \text{ and } \dfrac{\Delta\epsilon_y}{\epsilon_y} = 5\%\left(\dfrac{T_y\,[\text{mrad}]}{0.23}\right)^2 \text{ for the high luminosity parameters,} \end{cases}$$

(see the dot-dashed curves in Fig. 3 and 4).

[1] For a given accelerating gradient, the RF phase is adjusted to minimize the single-bunch RMS energy spread at the linac exit (short-range longitudinal wakefield compensation). For the high luminosity parameters, the optimum value of the RF phase, given in Tab.1, is slightly different from the one given in Ref. [5].

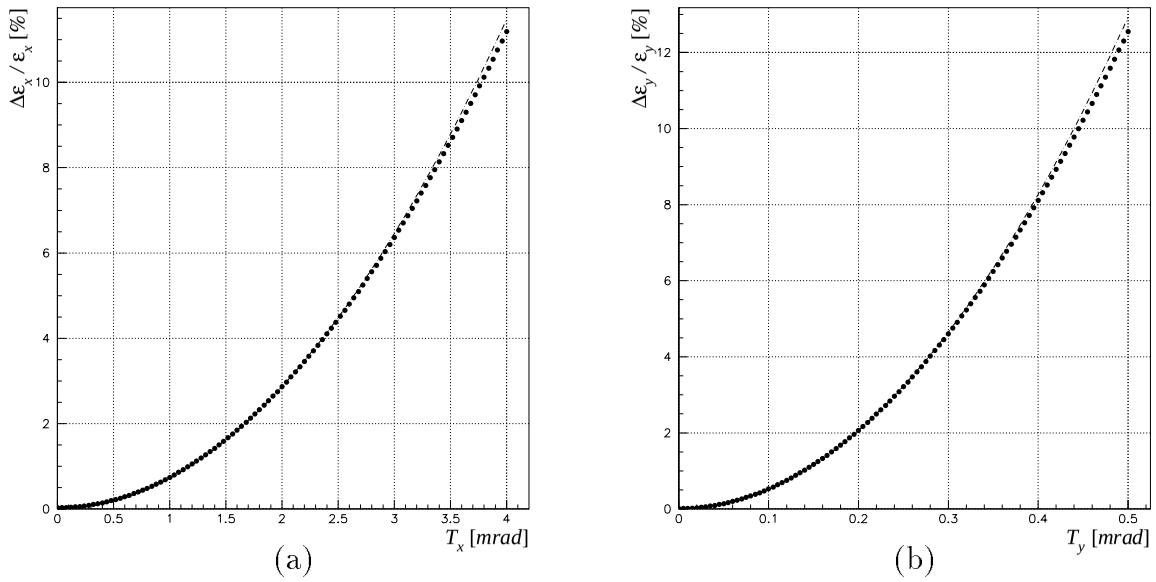

Figure 3: CDR beam parameter set: horizontal (a) and vertical (b) single-bunch emittance dilution at the TESLA linac exit versus T_x and T_y; one-to-one correction applied; the dot-dashed lines are parabolic fits of the numerical results obtained.

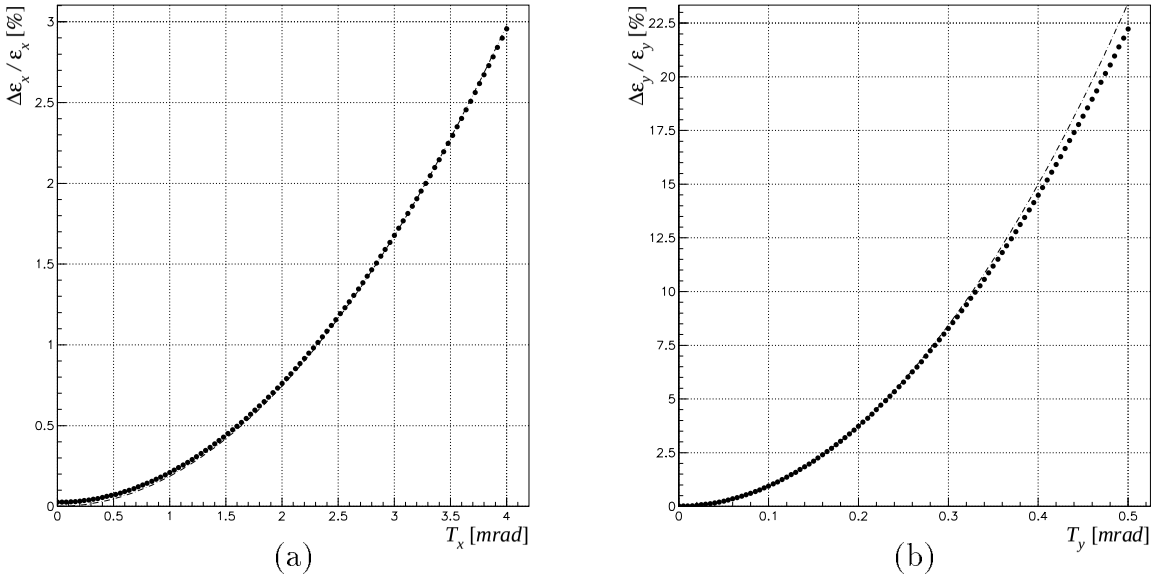

Figure 4: High luminosity beam parameter set: horizontal (a) and vertical (b) single-bunch emittance dilution at the TESLA linac exit versus T_x and T_y; one-to-one correction applied; the dot-dashed lines are parabolic fits of the numerical results obtained.

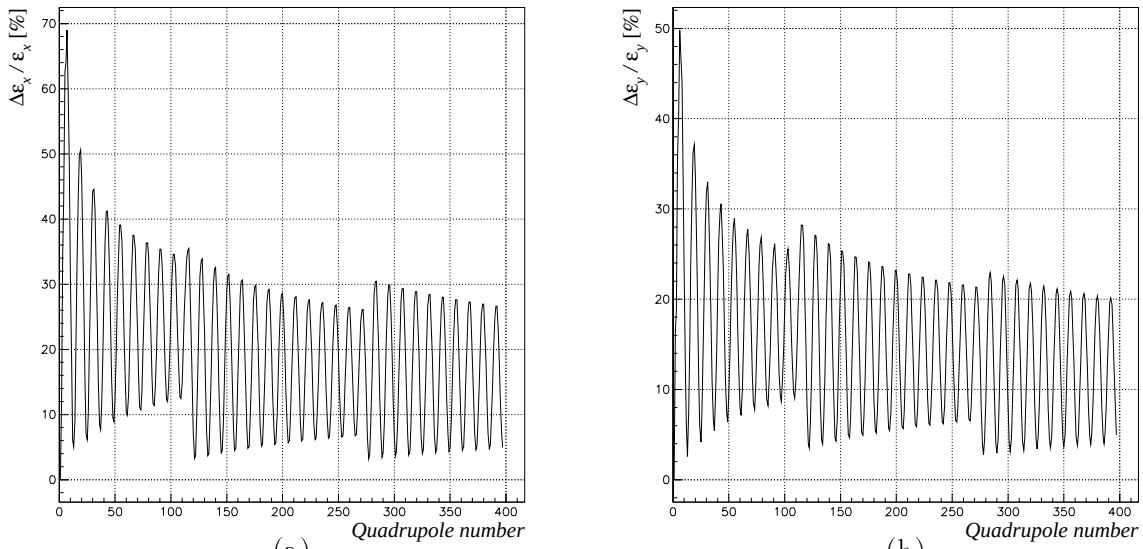

Figure 5: High luminosity beam parameters: horizontal (a) and vertical (b) single-bunch emittance dilution along the TESLA linac; one-to-one correction applied; $T_x = 5.19$ mrad and $T_y = 0.23$ mrad (tolerance values).

If the tolerance criterion is a relative emittance dilution lower than 5 %, the previous expressions show immediately that the measured values for T_x and T_y do not overstep the TESLA 500 specifications.
The emittance growth generated by RF-steering can be explained as follows:

1. the *slope* of the RF kick over the bunch length induces an head-tail effect proportional to $T \sin(\phi_0 + \phi_{\rm rf})\, \omega_{\rm rf}\, \sigma_z$ (σ_z and $\omega_{\rm rf}$ are the bunch length and the RF frequency respectively).

2. since the RF kick *averaged* over the bunch distribution is not zero, the beam trajectory remains off-axis even after correction (except at the BPM location), so that its emittance is also deteriorated by wakefield and chromatic effects (contribution proportional to $T \cos(\phi_0 + \phi_{\rm rf})$).

Nevertheless, since the direction and the magnitude of these deflections are approximatively equal from cavity to cavity (unlike the ones generated by random misalignments of the linac components), one expects, as a result of betatronic oscillations of the beam, that the transverse emittances oscillate along the linac instead of growing in a continuous way. More precisely, let us consider for instance two cavities C1 and C2 of the TESLA linac separated the one from the other by a phase advance of 180°. If the beam energy gain was completely negligible between these two cavities (and by assuming the same accelerating gradient in cavities C1 and C2), the two RF-kicks would then cancel each other at the level of the cavity C2 (that is no emittance growth). As illustrated below, this compensation exists effectively but remains partial because of the beam acceleration and also of the dipole wakefields excited between the two cavities previously considered. Fig. 5 shows

the horizontal and vertical single-bunch emittance dilution all along the TESLA linac for the high luminosity beam parameters. The emittances are calculated at the center of each quadrupole. As expected, the distance between an emittance maximum and its following minimum corresponds exactly to six quadrupoles, i.e. to a phase advance of $3 \times 60^\circ = 180^\circ$. The effect is clearly generated in the beginning of the linac where the acceleration of the beam is not negligible with respect to its average energy. The compensation previously mentioned is then not perfect; nevertheless, in order to take advantage of it, the total number of FODO cells in the last sector has been optimized (modulo 6) in such a way that the last quadrupole of the linac coincides with a minimum of emittance growth.

4 Conclusions

Rf kick	Measured values	Theoretical values	Tolerances for TESLA 500	
			CDR parameters	High luminosity parameters
T_x [mrad]	0.32 ± 0.03	0.18	2.64	5.19
T_y [mrad]	0.08 ± 0.03	0.00	0.31	0.23

Table 2: Factors T_x and T_y: measurements, theoretical values and tolerances for TESLA 500.

The main results obtained in this paper are summarized in Tab.2. The agreement between the measurements and the theoretical values expected for T_x and T_y is not very accurate. Consequently, it is important to repeat this experiment during the next run of TTF in order to check the validity of the experimental results obtained.
With the current measurement, these values are lower than the tolerances computed for TESLA 500, both for the CDR and for the high luminosity beam parameters.

References

[1] S. Fartoukh. *RF steering experiments on TTF.* DAPNIA/SEA-98-02 & TESLA-Note 98-01, Feb. 1998.

[2] M. Zhang and Ch. Tang. *Beam Dynamic Aspects of the TESLA Power Coupler.* TESLA-Note 98-17, July 1998.

[3] We thank M. Zhang for making us aware of this point.

[4] R. Brinkmann. *High Luminosity with TESLA-500.* TESLA-Note 97-13, August 1997.

[5] *Conceptual Design of a 500 GeV e+e- Linear Collider with Integrated X–ray Laser Facility.* DESY 97–048.